Validation of Numerical Modeling of Air Infiltration through Building Entrance Doors

Sherif Goubran, Dahai Qi, Wael F. Saleh, Liangzhu (Leon) Wang, Radu Zmeureanu

Department of Building, Civil and Environmental Engineering, Concordia University, Quebec, Canada

ABSTRACT

Air infiltration through building entrance doors has been the focus of many studies due to the significant effect infiltrated air has on the buildings' energy performance. Air infiltration models were developed for the double swing single and vestibule doors based on previous studies. It was concluded that vestibules doors are effective in reducing air infiltration. Currently vestibules are required as an energy saving measure for most commercial buildings. Our recent studies were focused on investigating the effectiveness of different entrance doors in reducing air infiltration in buildings. This paper presents the results from a preliminary effort in our recent studies: the experimental validation of the numerical modeling of air infiltration through single doors (double swing) using computational fluid dynamics (CFD). A reduced scale experimental chamber was built and the experimental setup was modeled in CFD. The volumetric airflow rates to the chamber were controlled and the resulting pressure differences across the door were measured and compared to the CFD results as well as existing sources in the literature. The experimental, numerical and theoratical results were found to be close and the modeling methods were validated.

INTRODUCTION

Air infiltration is the uncontrolled inward leakage of outdoor air into buildings through cracks in the building envelope or through large openings such as doors. Air leakage or movement in or out of buildings is mainly caused by the pressure difference across the various building enclosure elements (ASHRAE, 2010). The building sector (residential, institutional and commercial buildings) consumes about 41% of the primary energy use in the USA. It was estimated that air infiltration can, on average, account for up to 13% of the heating loads in U.S. office buildings (Emmerich & Persily, 1998; Wang, 2013). New studies confirm that with the increase of efficiency of equipment and building envelope, the relative percent energy loss due to air infiltration is becoming more significant (in relation to the total energy losses) (Deru, Field, Studer, & Benne, 2011; Ng, Emmerich, & Persily, 2014). Thus in modern and well insulated commercial buildings a larger portion of the heat losses are contributed to air infiltration; air infiltration is responsible for about 25% of the building heating loads for new buildings (Emmerich & Persily, 1998). With tight building envelopes, the major sources of air infiltration that remain in buildings are the exterior openings (doors and windows) (Cho, Liu, & Gowri, 2010; Emmerich & Persily, 1998; Ng et al., 2014).

Yuill conducted one of the pioneer studies on a 2.44 m × 2.44 m × 1.30 m (L × W × H) chamber to estimate infiltration rates for automatic doors based on door usage frequency, configuration, and pressure differences across the door (G. Yuill, 1996). Yuill developed infiltration models based on the orifice equation, that are still widely used in estimating the air infiltration through doors (ASHRAE, 2009). For a specific door opening angle and door configuration, Yuill experimentally measured the discharge coefficients and flow exponents needed to calculate the infiltration through the door (G. Yuill, 1996). It was found that a building entrance with a vestibule leads to smaller discharge coefficient, C_D, therefore less infiltration, than without it. Based on these findings, many energy codes, namely the American Society of Heating, Refrigerating and Air-Conditioning Engineers (ASHRAE) Standard 90.1 – Energy Standard for Buildings Except Low-Rise Residential Buildings and the International Energy Conservation Code, have opted to require fitting main entrances of commercial buildings with vestibule doors. More specifically, ASHRAE Standard 90.1 (Addendum 'q' to ASHRAE 90.1 - 2007 vestibule) requires vestibules to be installed in almost all types of building entrances located in climate zones 3 to 8 (ASHRAE, 2007).

Furthermore, Yuill was able to develop the overall door infiltration coefficient, C_A, based on the experimental data and field observation that can relate the infiltration rates to the door usage frequency, P_h. The coefficient C_A is calculated for a full door operation cycle (from the door fully closed to fully open then closed again). The model also uses a pressure factor, R_p, which depends on the building height and outdoor temperature condition. Using a series of charts available in ASHRAE (ASHRAE, 2009), an estimate of the infiltration rates through single and vestibule door can be calculated using Eq. (1).

$$Q = C_A \, A \, R_p \tag{1}$$

where
Q is the infiltration rate through the door with a specific door usage rate;
C_A is the overall average door coefficient for a specific door usage frequency - obtained from (ASHRAE, 2009);
R_p is the pressure factor for a specific building and outdoor condition - obtained from (ASHRAE, 2009);
A is the door opening area.

Another solution to restrict air infiltration is the use of air curtains. The units, typically made of a fan and casement with a jet outlet, are used as barriers in many applications. Air curtains have been used as a barrier to reduce fuel consumption in disposal burners (Schapiro 2002), to control respirable dusts in the mining industry (Kissell and Colinet 2001), to preserve low temperatures in cold storage rooms and food display cabinets (Goncalves et al. 2012), and to block smoke dispersion during fires in buildings and transportation tunnels (Krajewski and Sztarbala 2011) (Elicer-Cortes et al. 2009; Felis et al. 2010).

Even though literature on air curtains has been available for a while, it mainly focused on closed room applications with high temperature differences rather than entrance doors (open to the exterior). The series of studies conducted by Wang et al. (Goubran, Qi, & Wang, 2015; Qi, Goubran, Zmeureanu, & Wang, 2015; Wang & Zhong, 2014a, 2014b; Wang, 2013) aimed to quantify the impact of air curtain doors on the whole building energy usage. Using mainly numerical simulations, Wang's study (Wang, 2013) concluded that air curtain doors reduce significantly the air infiltration and energy loses through entrance doors when compared to vestibule or single doors under the same conditions. It was also concluded that air curtain doors can reduce whole building energy usage when compared to vestibule doors.

Among our current efforts to further study air curtains, an in-depth research was designed to validate the numerical modeling of air infiltration through entrance doors. This paper presents one of the preliminary efforts of the experimental validation of CFD modeling of infiltration through a double swing door in a reduced scale experimental chamber. Experimental and numerical results from this study are compared to the infiltration rates obtained through the models developed by Yuill's theoretical model (G. Yuill, 1996).

METHODOLOGY

A reduced scale experimental chamber (1/3 of a real chamber scale) was designed and constructed at Concordia University Building Environmental lab (hereafter the CUBE chamber) to be similar in dimensions as that used by Yuill (1996). The chamber and its surroundings were then modeled numerically. The infiltration through the chamber door (double swing single doors, hereafter single door) was measured, simulated and then compared to the theoretical infiltration obtained using Yuill's model (G. Yuill, 1996). Yuill reported for single doors open at 90° a flow coefficient of 0.62 and a flow exponent of 0.49 (G. K. Yuill, Upham, & Hui, 2000; G. Yuill, 1996) and the air infiltration was calculated based on Eq. 2.

$$Q_{angle} = C_{D,angle} \, A \sqrt{\frac{2\Delta P}{\rho}} \tag{2}$$

where
Q_{angle} is the infiltration rate through the door open at a specific angle;
$C_{D,\,angle}$ is the door discharge coefficient at a specific angle;
A is the door opening area;
ΔP is the pressure difference across the door, and
ρ is the air density.

The following two sections will present the detailed experimental and numerical simulation methodologies.

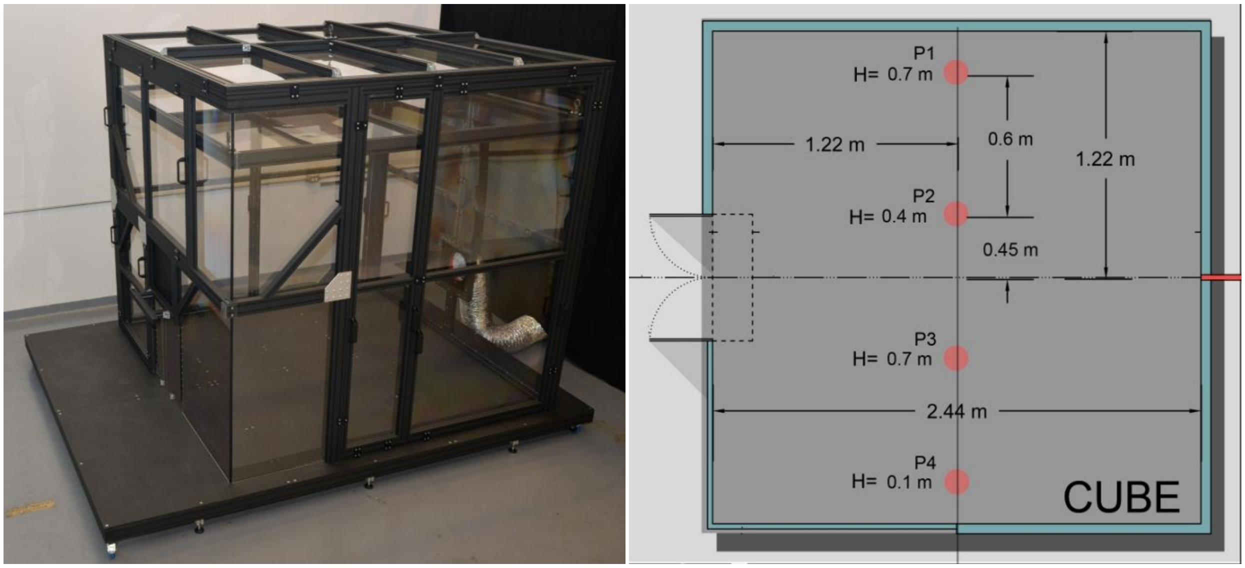

Fig. 1. The CUBE experimental chamber – 3D view (left, picture courtesy from MËKANIC) and location of the pressure reading points/nodes (right).

EXPERIMENT

An experimental chamber of 2.44 m × 2.44 m × 1.30 m (L × W × H) was designed for this study (a picture of the chamber is presented in Fig. 1). The chamber was built using Lexan panels supported by an aluminum frame. The chamber is equipped with a double swing door (made of hinged Lexan panels) of 0.61 m × 0.71 m (W × H).

The chamber is equipped with a duct blaster fan ("Minneapolis Duct Blaster® System) placed at the opposing wall to the door at a height of 0.65 m (measured from center of the duct opening to the ground). The fan is used to create a given pressure difference, ΔP, across the door between inside and outside by depressurization or pressurization. Based, on the conservation of mass, the mass air flow through the door is equal to the flow through the duct blaster fan. The duct ending in the chamber (at the interior of the chamber) was equipped with an air diffuser to avoid direct flow through the door. The inside pressure of the chamber was averaged based on four (4) points at the chamber's mid-depth plane (Fig. 1). The averaging of the four measurement points was done by joining the four tubes together to be used as one input in the pressure transducer (thus obtaining 1 averaged pressure reading). The pressure difference measurements were obtained using DG-700 model pressure transducer ("DG-700 Pressure and Flow Gauge). The pressure difference across the door was calculated based on the difference between the pressure inside and outside (far from the chamber).

For each fan flow rate, pressure difference was calculated based on an average of two measurements. Since the chamber would have airflow at significant speed, the tube endings were fitted with protectors to ensure only the static pressure (rather than the stagnation pressure) is measured (Fig. 2). It is important to note that pressure differences were limited due to the measurement range of the equipment (Table 2). The temperature of the laboratory where the CUBE is installed were recorded during the testing and averaged at 23 °C, which was used to calculate the air density.

Table 2. Experimental limits of pressure and air flow conditions

	Minimum	Maximum
Pressure difference (Pa)	-0.85	1.3
Air flow rate (m^3/s)	-0.24	0.38

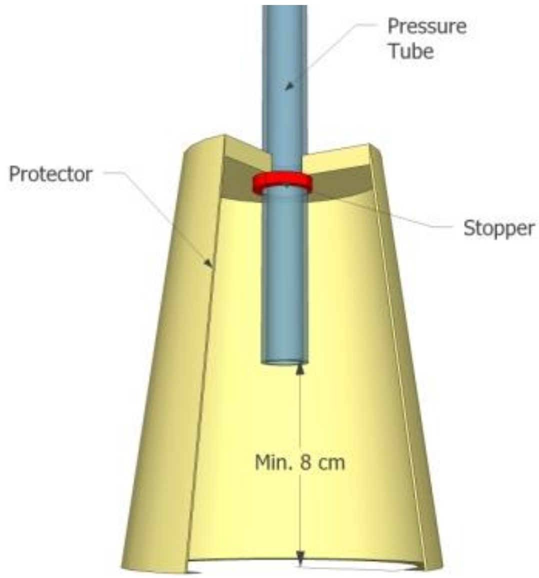

Fig. 2. Tube ending protection for static pressure measurements.

A total of 10 averaged data points for the air flows and pressure differences were recorded (20 measurements were acquired with two data points for each flow condition).

The average error for the pressure difference measurements was calculated to ± 1.3% or ± 0.21 Pa. Also, based on tests conducted on the air tightness of the chamber (using depressurization testing for 1 pressure condition) and the error range of the equipment used, the average bias error for the air flow measurements (for all the experiments conducted) was calculated to be ± 9% or ± 0.02 m^3/s.

CFD SIMULATION

The geometry of the modeled chamber and the surroundings are shown in Fig. 3. The pressure generated by the fan is modeled as one of the boundary conditions. The small hole that is far from the chamber is modeled as the pressure outlet in the boundary conditions.

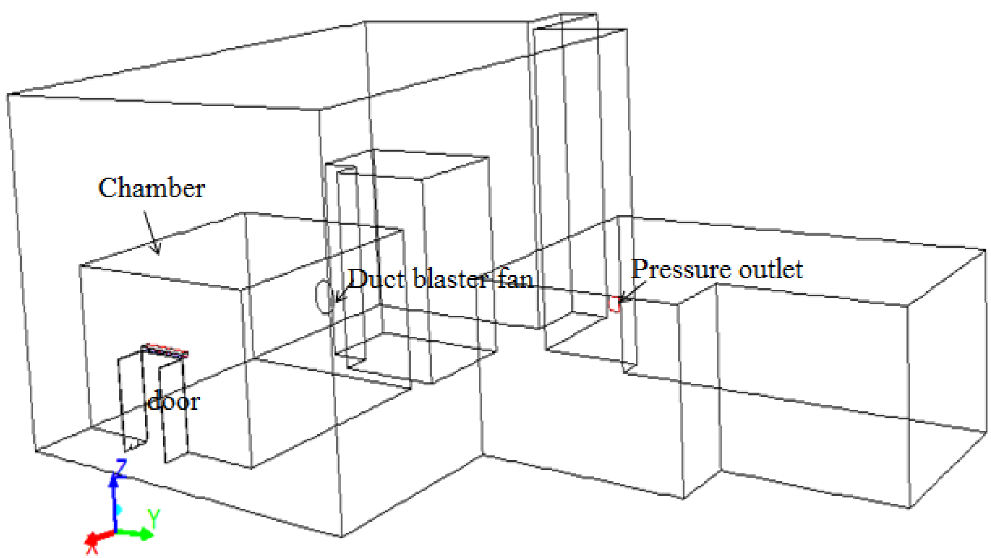

Fig. 3. CFD model of experimental chamber and its surroundings.

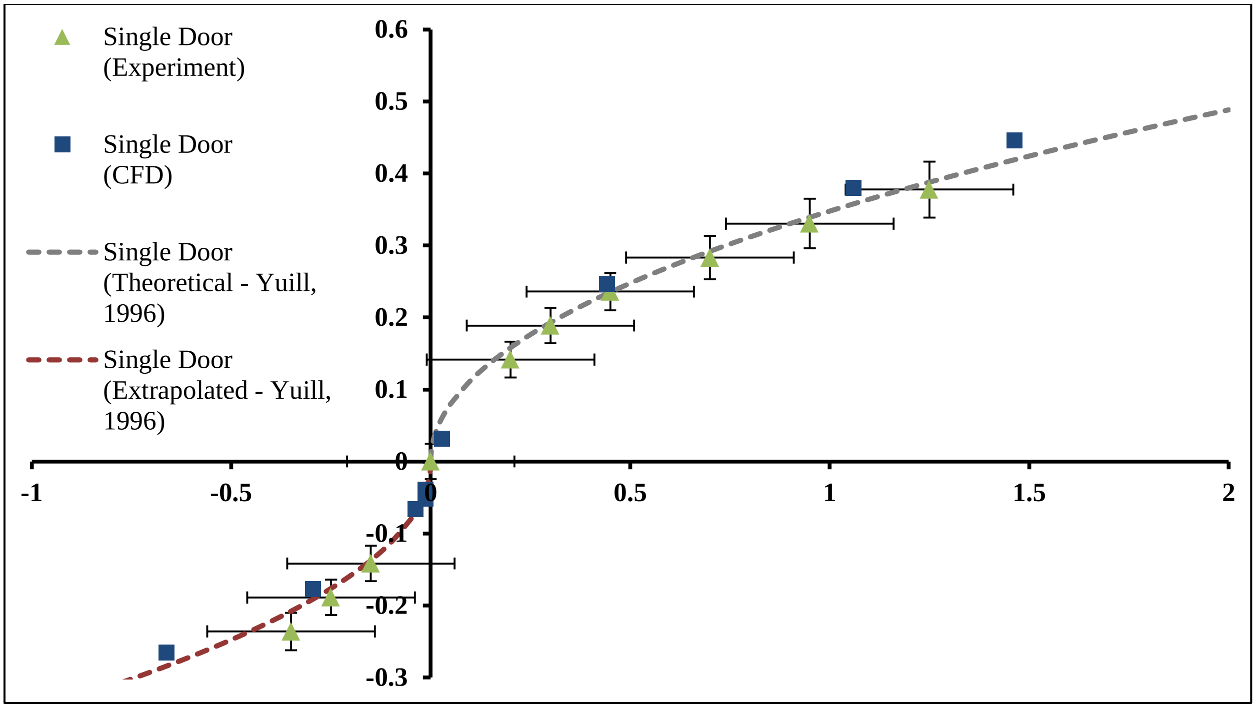

Fig. 4. Infiltration rates and pressure difference obtained experimentally and from simulations in comparison to the data calculated based on Yuill's model (G. Yuill, 1996).

The volumetric flow rate was controlled to match and cover the flow and pressure ranges presented in Table 2. In the numerical simulations, the volumetric flow rate ranged between -0.27 ~ 0.45 m^3/s creating a corresponding pressure difference of 27~76 Pa. Similar to the experimental setup, the CFD model also includes a diffuser in front of the duct outlet. The grid size near the door opening is 0.016 m × 0.016 m. In the far side of the domain away from the fan a coarser grid is used with the size of 0.064 m × 0.064 m. Outside the chamber a 0.128 m × 0.128 m grid is used. The total number of the grids is about 1.6 million.

For this paper, a total of ten CFD simulations by using ANSYS FLUENT 14.0 (ANSYS, 2011) were performed to simulate the air infiltration through the open double swing door. The CFD simulations are considered at steady state based on the standard $k-\varepsilon$ model and the pressure-velocity coupling adopts the SIMPLE algorithm. Standard wall function is applied as the near wall treatment. The details of the CFD simulations are presented in Table 3.

The pressure difference across the door between outside and inside of the chamber, ΔP, in Eq. (2) is calculated based on the average pressure the chamber, P_i (based on the four - 4 - points/nodes presented in Fig. 1), and the outside pressure at a location undisturbed by the flow of the chamber, P_o, which is used as the reference pressure (approximately 0 Pa).

Table 3. CFD simulation settings.

Chamber	Size	2.44 m × 2.44 m × 1.30 m (L × W × H)
Door	Door size	0.61 m × 0.71 m (W × H).
	Door opening angle	90^0 (fully open)
CFD	Total grid number	1,600,000
	simulation	Steady state
	Turbulence model	Standard $k-\varepsilon$ model
	Boundary conditions	Pressure drop across the fan from outside to inside chamber: 27~76 Pa; Pressure outlet far away from the chamber

RESULTS

The experimental flow rates and pressure differences (two pressure points for each flow condition, ΔP_1 and ΔP_2) are presented in Table 4. The two pressure measurements were obtained for the same flow rate and are used to ensure the repeatability of the measurements. These experimental pressure readings are then averaged and presented in Fig. 4. The pressure differences and infiltration rates obtained from the numerical simulation (CFD) for the tested door are presented in Table 5. The comparison between the experimental, CFD modeling and theoretical results (G. Yuill, 1996) are presented in Fig. 4. The bias error of the experimental data is also represented in Fig. 4

Table 4. Experimental measurements for airflow and pressure differences.

Q (m^3/s)	ΔP_1	ΔP_2
0.38	1.2	1.3
0.33	1	0.9
0.28	0.7	0.7
0.24	0.5	0.4
0.19	0.3	0.3
0.14	0.2	0.2
0	0	0
-0.14	-0.2	-0.1
-0.19	-0.3	-0.2
-0.24	-0.4	-0.3

Table 5. CFD results for the airflow and pressure differences

Q (m3/s)	ΔP
0.45	1.5
0.38	1.1
0.25	0.44
0.032	0.029
0	0
-0.039	-0.013
-0.052	-0.013
-0.067	-0.037
-0.18	-0.294
-0.27	-0.661

DISCUSSION

The experiments and simulations were conducted for both positive and negative pressure difference conditions. This differs from the experimental setup used by Yuill (1996) which focused mainly on the positive pressure difference range (studying air infiltration through the door rather the air exfiltration). However, Yuill's study (1996) was the main study found to report the coefficients for these doors, the discharge coefficients he proposed were used to extrapolated in the infiltration curve in the negative ΔP range seen in Fig.4.

The positive pressure difference range in Fig. 4 indicates that the inside of the chamber has a lower pressure than the outside (i.e. the chamber is depressurized). Under this condition, air infiltrates through the door into the chamber. The negative pressure difference range in Fig. 4 indicates that the inside of the chamber has a higher pressure than the outside (i.e. the chamber is pressurized). Under this condition, air exfiltrates from the inside of the chamber to the outside. In both pressure difference ranges, both the CFD simulation results and the experimental measurements agree well and are in close proximity to range to the infiltration curve obtained by Yuill's model (G. Yuill, 1996). Based on the data presented the average calculated flow coefficient for the experimental results is 0.62 which is similar to that obtained by Yuill. The average difference between the experimental results and the infiltration curve obtained by Yuill's model is 3.48% for all the tested points. The CFD simulation results show a higher difference when compared to Yuill's model with 11.2% error for all the 10 conditions simulated.

It can be observed in Fig. 4 that in the positive pressure difference range investigated, the experimental and CFD results agree better with each other than with the curve obtained by Yuill's model (G. Yuill, 1996). In the negative pressure difference range, bigger differences can be observed between Yuill's model and the results of this study. In the negative pressure difference range, the difference between Yuill's infiltration curves for the single door and the experimental results is 5.9% based on four measurements (this value is much higher than the average difference). This large difference could be due to higher errors in the pressure measurements in the chamber due to the airflow cause by the fan. However, it can be related to the fact that the model developed by Yuill was solely based on the infiltration (depressurized chamber condition). Further analysis of the experimental results show that in the positive pressure difference range the calculated flow coefficient C_D is 0.60 (based on six measurements) and in the negative pressure difference range it is closer to 0.67 (based on three measurements). This analysis indicates that the airflow in the chamber can experience different resistance based on the direction of the flow through the door.

As indicated in the methodology section of this paper, the pressure difference and flow rate ranges were limited by the fan used. In order to obtain conclusions that can be generalized for buildings in operation, the pressure difference range (both in the positive and negative ranges) should be extended to higher values that correspond to the actual pressure differences in the field - an average number is reported to be ± 10 Pa (Wang, 2013).

However, based on the data presented, the CFD modeling method used in this paper is accurate in capturing the infiltration through the door when compared to the experimental results. Both the experimental and numerical results generally support Yuill's findings and method for calculating air infiltration through fully open double swing doors. Based on these findings, further investigation can be conducted on the flow conditions (the coefficient and flow exponent) for the exfiltration conditions. Meanwhile, the investigation can be extended to validate the numerical modeling of other entrance door types such as the doors equipped with air curtain.

CONCLUSIONS

This paper introduces the validation of the CFD modeling of air infiltration through double swing doors by experiments. A reduced scale experimental chamber was built, which was simulated by CFD. The volumetric airflow rates were controlled by the duct blaster fan, resulting in pressure differences across the door. The calculated infiltrated flow rates through the door by CFD were compared to the measured results. Both the experimental and simulation results were evaluated against the infiltration rates obtained by Yuill's model (G. Yuill, 1996).

Based on the experimental results gathered from the chamber, it is concluded that the measurements reported by Yuill (G. Yuill, 1996) for the flow coefficient and exponent for the double swing door open at 90° are accurate for the pressure difference range tested. It is also concluded that the CFD modeling method used is valid and is able to accurately capture the infiltration through the doors of the chamber under the reported conditions.

Based on the data gathered and presented in this paper, the experimental study of airflow through building entrance doors can be extended to investigate and validate the modeling of infiltration through different entrance door conditions: e.g. vestibules, revolving doors or doors with air curtains.

ACKNOWLEDGEMENT

The authors acknowledge the financial and technical support from the Air Management and Control Association (AMCA), Mars Air Systems, Berner International, Powered Aire and InterCode Incorporated. The author would also like to thank MËKANIC team for the construction of the experimental chamber as well as providing professional images for the experimental setup used in this paper.

REFERENCES

ANSYS. (2011). *ANSYS FLUENT User's Guide – Release 14.0*. *ANSYS*. Canonsburg, PA.

ASHRAE. (2009). *ASHRAE Handbook–Fundamentals*. Atlanta: American Society of Heating, Refrigerating and Air Conditioning Engineers, Inc.

ASHRAE. ASHRAE standard 90.1-2010: Energy Standard for Buildings Except Low-Rise Residential Buildings, ASHRAE/IESNA Standard (2010).

Cho, H., Liu, B., & Gowri, K. (2010). Energy Saving Impact of ASHRAE 90.1 Vestibule Requirements: Modeling of Air Infiltration through Door Openings. *Pacific Northwest National Laboratory*, (November). Retrieved from http://www.pnl.gov/main/publications/external/technical_reports/PNNL-20026.pdf

Deru, M., Field, K., Studer, D., & Benne, K. (2011). US Department of Energy commercial reference building models of the national building stock. *National Laboratory of the U.S. Department of Energy*, (February 2011). Retrieved from http://www.nrel.gov/docs/fy11osti/46861.pdf

DG-700 Pressure and Flow Gauge - The Energy Conservatory. (n.d.). Retrieved December 4, 2015, from http://products.energyconservatory.com/dg-700-pressure-and-flow-gauge/

Emmerich, S. J., & Persily, A. K. (1998). Energy Impacts of Infiltration and Ventilation in U.S. Office Buildings Using Multizone Airflow Simulation. In *IAQ and Energy 98 Conference* (pp. 191–203). New Orleans.

Goubran, S., Qi, D., & Wang, L. (Leon). (2015). Annual Energy Saving Impact of Air Curtains in Commercial Reference Buildings. In *ISHVAC-COBEE* (p. 8). Tianjin.

Minneapolis Duct Blaster® System - The Energy Conservatory. (n.d.). Retrieved December 4, 2015, from http://products.energyconservatory.com/minneapolis-duct-blaster-system/

Ng, L. C., Emmerich, S. J., & Persily, A. K. (2014). An Improved Method of Modeling Infiltration in Commercial Building Energy Models. In *2014 ASHRAE/IBPSA Building Simulation Conference* (pp. 308–315). Atlanta.

Qi, D., Goubran, S., Zmeureanu, R., & Wang, L. L. (2015). Effect of People on Infiltration of Building Entrance with Air Curtains. In *ISHVAC-COBEE* (p. 9). Tianjin.

Wang, L. (Leon). (2013). *Investigation of the Impact of Building Entrance Air Curtain on Whole Building Energy Use*. *Air Movement and Control Association*. Retrieved from http://www.amca.org/UserFiles/file/Energy Initiative Web Pages/Air Curtain Study.pdf

Wang, L. (Leon), & Zhong, Z. (2014a). An approach to determine infiltration characteristics of building entrance equipped with air curtains. *Energy and Buildings*, *75*, 312–320.

Wang, L. (Leon), & Zhong, Z. (2014b). Whole Building Annual Energy Analysis of Air Curtain Performance in Commercial Building. In *eSim*. Ottawa.

Yuill, G. (1996). *Impact of High Use Automatic Doors on Infiltration*. *ASHRAE Research Project 763-TRP*. Pennsylvania.

Yuill, G. K., Upham, R., & Hui, C. (2000). Air leakage through automatic doors. *ASHRAE Transactions*, *106*(2), 145–160.